Boundary selectivity of crack paths in corrosion fatigue of stainless steel

Conference or Workshop Item

BOUNDARY SELECTIVITY OF CRACK PATHS IN CORROSION-FATIGUE OF STAINLESS STEEL

S.M. Northover* and C.R.M. Grovenor~

*The Open University in the South, Foxcombe Hall, Boars Hill, Oxford OX1 5HR, ~Department of Materials, University of Oxford, Parks Road, Oxford, OX1 3PH, UK.

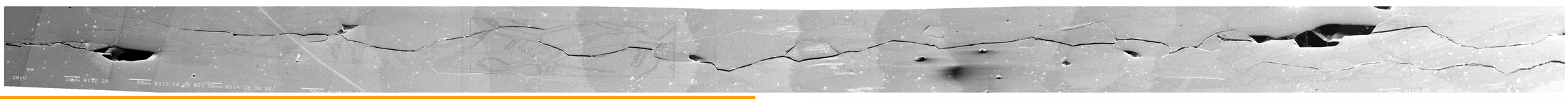

Introduction

Although austenitic stainless steels are highly resistant to corrosion in many environments they are sometimes susceptible to intergranular stress corrosion cracking and corrosion fatigue. This susceptibility varies from boundary to boundary with coherent twins in particular being apparently immune. This led to the suggestion that a boundary's susceptibility to cracking could be related to the proximity of its misorientation to one associated with a high density of coincident lattice sites. This has prompted attempts to modify the grain boundary character distribution to give a higher proportion of 'special' ie crack-resistant boundaries. Gertsman and Bruemmer (1) studied grain boundary character along intergranular stress corrosion crack paths in austenitic alloys in an attempt to establish whether resistance to cracking could be associated with a low value of reciprocal coincident lattice site density (Σ) They concluded that under the conditions they used only Σ3 twins could be regarded as special and that the occurrence of other low-Σ boundaries along the crack path was no different from that expected from their frequency in the overall grain boundary population. Gertsman and Bruemmer were able to study only a relatively small number of cracked boundaries and the present study examined a much longer corrosion fatigue crack to find if under different conditions the crack path discriminated between 'general' boundaries and any low-Σ boundaries other than Σ3.

Experimental Details

The composition of the specimen was given as:

C	Cr	Ni	Mn	Mo	Si	Cu	S	P	Co	V
0.054	18.2	8.08	1.56	0.52	0.3	0.36	0.02	0.034	0.08	0.04
Al	W	Nb	Ti	Fe						
0.01	<0.05	<0.01	<0.01	balance						

Prior to testing the compact tensile specimen was sensitised by holding at 650°C for 24 hrs

Crack Growth

The corrosion fatigue crack was grown at open circuit potential in non refreshed, aerated 0.1 M potassium tetrathionate acidified to pH 1.5 at room temperature (22 ± 2°C) in accordance with ASTM E647 A1. Starting with a fatigue pre-crack at a stress intensity factor range (ΔK) of approximately 15 MPa√m, the crack was grown at constant load (K increasing) with a sinusoidal wave form at a frequency of 0.01Hz and a load ratio of R = 0.1 to a length of approximately a/w = 0.7

Specimen Preparation

A slice approx 1.5mm thick was cut from the compact tensile specimen in the plane containing the loading and crack growth directions and from this was machined a 10 mm dia. disk containing the crack. This was mounted in carbon-filled thermosetting resin and mechanically polished to 0.25µm. Final polishing was with colloidal silica. The disk was then removed from the mount and fixed to an SEM stub with silverdag.

EBSD analysis

Electron backscattered diffraction analysis was carried out systematically along the whole length of the crack using a JEOL 6480 LV SEM at 30kVand HKL analysis software to create 2D orientation maps with a point separation of 2 microns. For the majority of the mapping, "Smart mapping" was used to shorten the acquisition times. Three large areas (a total area of approximately 3 mm^2 containing more than 10,000 grains) well away from the crack were also mapped to act as a reference for the natural distribution of grain boundaries of different misorientations.

The specimen was then repositioned at 0° tilt for high resolution SEM imaging over the same area.

Figure 1. The composite SEM images at top and bottom of the poster show the full length of the crack after EBSD mapping. Several examples of grain dropout during polishing can be seen along the crack indicating the multi-branched 3D structure of this kind of crack.

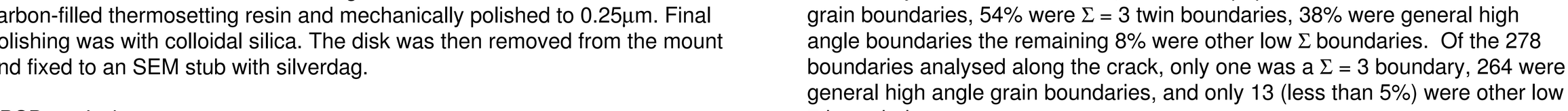

(1) Gertsmann, V.Y. and Bruemmer, S.M., Acta Materialia 49 (2001) 1589

Results

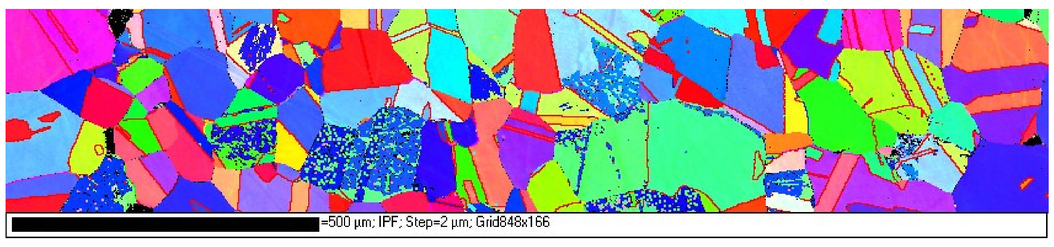

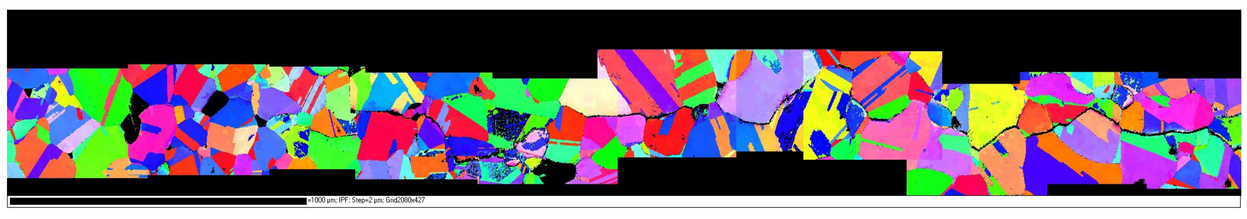

Figure 2. Top: A typical IPF map far from the crack
Bottom: A typical IPF map from a section of the crack

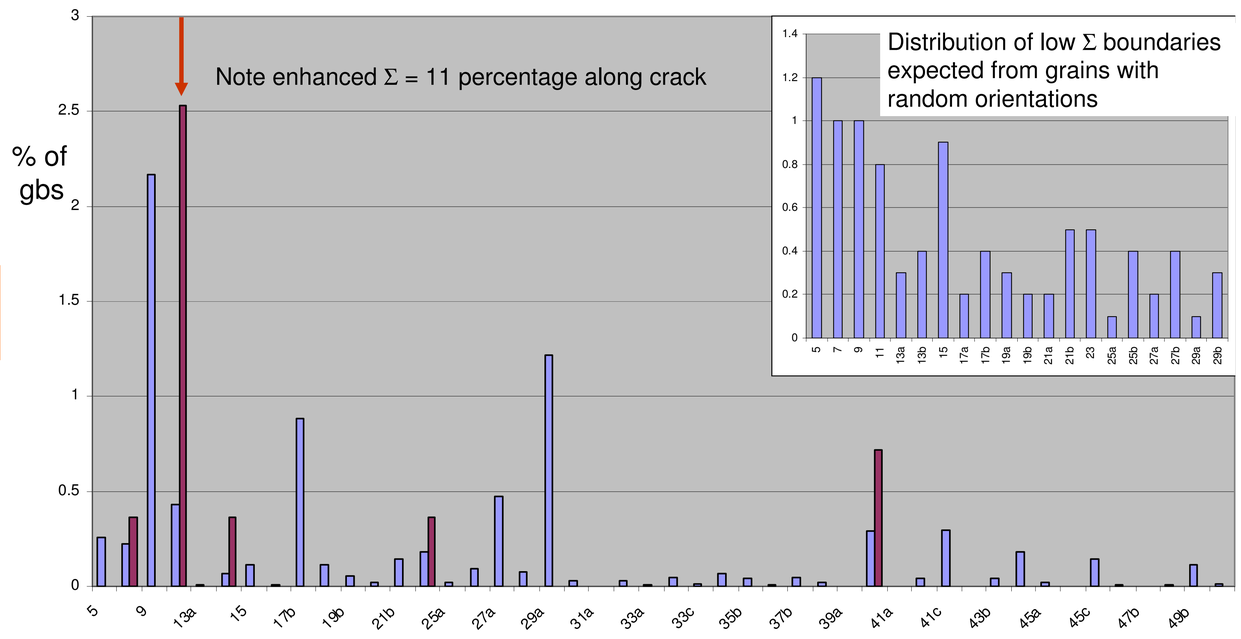

Figure 3: Percentage of identified grain boundaries with low Σ misorientations along the crack path (maroon) compared to the general boundary population (blue). The apparently high percentage of Σ = 29 boundaries in the general population is an artefact (see below).

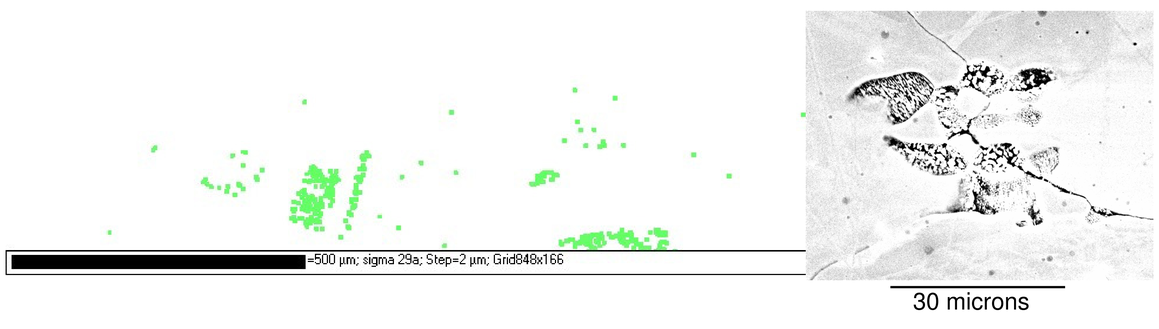

Figure 4: EBSD image from the same area as the top map in Figure2, highlighting areas identified by the software as being surrounded by Σ = 29 boundaries, but which are probably due to second phase areas as illustrated on the RHS.

From analysis of the EBSD data, of the bulk population of more than 40,000 grain boundaries, 54% were Σ = 3 twin boundaries, 38% were general high angle boundaries the remaining 8% were other low Σ boundaries. Of the 278 boundaries analysed along the crack, only one was a Σ = 3 boundary, 264 were general high angle grain boundaries, and only 13 (less than 5%) were other low Σ boundaries.

The chart in Figure 3 compares the measured percentages of grain boundaries with low Σ misorientations in the bulk material (blue) with those for the cracked grain boundaries (maroon). We note that the percentages in the bulk are measured as fractions of total line length of boundary, while at the crack the percentages are of numbers of boundaries. The main observation is that 7 of the 13 cracked low Σ boundaries were Σ = 11, a clear suggestion that this particular low Σ misorientation shows an enhanced propensity to crack under the conditions studied in this work.

Acknowledgements

The authors would like to thank Dr Brian Connolly of the University of Birmingham for supplying the cracked specimen and details of crack growth and Chris Salter of the University of Oxford for training on the SEM.